Ionic Basis of Arrhythmic Risk Biomarkers on Simulated Rabbit Ventricular Myocytes

L Romero, B Carbonell, B Trénor, JM Ferrero

Universidad Politécnica de Valencia (I3BH), Valencia, Spain

Abstract

Cardiac proarrhythmic risk can be estimated considering several biomarkers based on electrophysiological properties. The aim of this work is to identify the key ionic mechanisms predicting arrhythmia generation in rabbit hearts at the cellular level. For this purpose, the sensitivity of action potential (AP) duration (APD), AP triangulation, AP rate dependence and intracellular calcium and sodium levels to variations in transmembrane ionic current conductances was analyzed.

Simulations show that, in rabbit, APD is moderately influenced by changes in all repolarization current conductances, highlighting I_{NaK}, I_{CaL} and I_{Kr}. AP triangulation, however, is basically determined by I_{K1} and I_{Kr}. In addition, AP rate dependence is especially sensitive to I_{NaK}, I_{NaCa}, I_{Kr} and I_{CaL}. Furthermore, intracellular calcium and sodium levels are highly determined by I_{CaL}, I_{NaK} and I_{NaCa}.

1. Introduction

Cardiac arrhythmias are the main cause of mortality in developed countries. To predict proarrhythmic risk, several biomarkers based on cellular electrophysiological properties have been proposed in the literature [1]. Most of these biomarkers are related to action potential (AP) shape and duration, intracellular calcium and sodium concentrations, and their rate dependence.

Prolongation of the QT interval has traditionally been linked to Torsade de Pointes, a potentially mortal arrhythmia [2]. In addition, prolongation of AP triangulation has been related to early-afterdepolarizations appearance [1]. Furthermore, experimental investigations reveal the importance of sodium and calcium intracellular concentrations for arrhythmia generation [3].

It is also well known that alterations of rate dependent properties are key in arrhythmic episodes. Indeed, steep restitution curves are associated to AP alternans occurrence and wavefront breakup, which is a hallmark of ventricular fibrillation, a potentially mortal arrhythmia

[4]. Moreover, cardiac myocytes exhibiting a slow APD rate adaptation to sudden abrupt changes in cardiac pacing are prone to develop cardiac arrhythmias [5].

In this paper, a mechanistic investigation into the ionic basis of arrhythmic risk biomarkers of simulated rabbit ventricular myocytes is performed. For this purpose, the sensitivity of the main cellular biomarkers to modifications in the main transmembrane current conductances has been quantified using the Shannon et al. ventricular AP model [6]. This analysis is based on our previous study in human cardiomyocytes [7].

2. Methods

The electrophysiological activity of an isolated rabbit ventricular myocyte was simulated using the Shannon et al. ventricular AP model [6].

Four protocols, similar to those described in our previous work [7], were applied to the virtual rabbit myocytes in order to characterize the main arrhythmic risk biomarkers.

APD, AP triangulation and systolic intracellular calcium concentration ($[Ca^{2+}]_i$) were calculated after applying a train of 1,000 rectangular current pulses of 2 ms in duration and an amplitude of twice the diastolic threshold at a basic cycle length (BCL) of 400 ms. APD was considered at 90% repolarization and AP triangulation was defined as the difference between APD_{90} and APD at 60% repolarization (APD_{60}).

APD restitution curves were obtained using the standard (S1S2) and the dynamic restitution protocol. The S1S2 restitution protocol consisted of a train of 10 rectangular current pulses (S1) at a BCL of 400 ms followed by an extra stimulus (S2) at coupling intervals ranging from 2,000 ms to 50 ms with a CI step of 1 ms. The S1S2 restitution curve was generated by plotting the APD_{90} versus the diastolic interval (DI) for each extra stimulus. The dynamic restitution curve describes the dependence of the steady state APD_{90} on the DI for BCLs ranging from 1,000 ms to 50 ms. The maximal slopes of both curves ($slope_{max,\ S1S2}$ and $slope_{max,DYN}$) were obtained.

In order to analyze the APD_{90} rate adaptation, the virtual rabbit cardiomyocyte was paced a BCL of 100 ms

for 8 minutes, then at a BCL of 600 ms for 8 minutes and finally the BCL was set back to 1000 ms for 8 minutes. The slow time constant (τ_{slow}) of the temporal APD_{90} adaptation to the accelerating rate was computed [7].

Finally, a frequency staircase protocol was applied to the myocytes to characterize the rate dependence of the steady state intracellular calcium and sodium ($[Na^+]_i$) concentrations. Ventricular myocytes were stimulated at increasing frequencies for 10 minutes, and systolic $[Ca^{2+}]_i$ and $[Na^+]_i$ levels were recorded for each pace and normalized to the respective values at 0.25Hz.

The sensitivity analysis was performed to investigate the impact of the maximal conductances of the main transmembrane currents on the selected arrhythmic risk biomarkers. Indeed, we analyzed the effect of the maximal conductance (G_{Na}) of the rapid sodium current (I_{Na}), the maximal conductance (G_{CaL}) of the L-type Ca^{2+} current (I_{CaL}), the maximal conductance (G_{Kr}) of the rapid component of the delayed rectifier current (I_{Kr}), the maximal conductance (G_{Ks}) of the slow component of the delayed rectifier current (I_{Ks}), the maximal conductance of the inward rectifier K^+ current (I_{K1}), the maximal activity of Na^+/K^+ pump (G_{NaK}) and the maximal activity of the Na^+/Ca^{2+} exchanger (G_{NaCa}). Simulations were run by varying one conductance by -30%, -15%, +15% and 30%, respectively, at a time.

Two indexes were used to quantify the influence of each conductance ("c") on each biomarker ("b"): percentage of change ($D_{c,b,a}$) and sensitivity ($S_{c,b}$). They were computed as follows:

$$D_{b,c,a} = \frac{\left(b_{c,a} - b_{control}\right)}{b_{control}} \cdot 100 \qquad (1)$$

$$S_{b,c} = \frac{\Delta D_{b,c,a}}{\Delta a} = \frac{D_{b,c,+30\%} - D_{b,c,-30\%}}{0.6} \qquad (2)$$

with $b_{c,a}$ and $b_{control}$ being the magnitude of the biomarker "b" when the conductance "c" is increased by "a" and under control conditions, respectively. In addition, relative sensitivities resulting from the normalization of the sensitivities ($S_{b,c}$) to the maximum absolute value of sensitivity obtained for that specific biomarker were considered.

3. Results

Figure 1 shows the relative sensitivities for all combinations of conductances and biomarkers using a gray scale. Negative sign means that conductance and biomarker vary inversely. Moreover, for each row, the maximum absolute sensitivity $S_{b,c}$ is also indicated as a percent value. As G_{Na} exerts an insignificant effect on the selected biomarkers, it was not included in this figure. Figures 2 and 3 illustrate the changes exerted in the biomarkers when ionic conductances are modified by

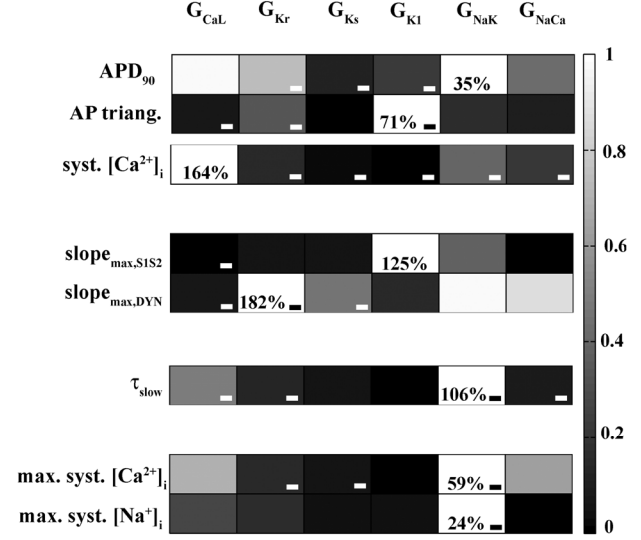±15% and ± 30%. These results are described in the next paragraphs.

Figure 1. Relative sensitivities of the arrhythmic risk to variations on ionic current conductances. Percentages in white boxes indicate the maximum absolute sensitivity of the property correspondent to that row. Negative sign indicates an inverse relationship between biomarker and conductance.

Steady state properties

Our simulations show that, in rabbit, APD_{90} is moderately sensitive to changes in all repolarization current conductances, especially I_{NaK} (S = 35%), I_{CaL} (S = 33%) and I_{Kr} (S = -26%). Simulated APD_{90} is 177.2 in control whereas experimentally reported values are slightly larger varying between 200 ms and 250 ms [8].

Simulated rabbit AP triangulation, is strongly dependent on I_{K1} (S = -70%) and I_{Kr} (S = -24%), although to a lesser extent. In our simulations, control AP triangulation is 18.9 ms, which is smaller than the electrophysiological values reported in the scientific literature namely from 26 ms [9] to 32 ms [8].

Regarding the steady state of systolic $[Ca^{2+}]_i$, our simulations reveal that I_{CaL} plays a key role (S = 164%). I_{NaK} (S = -65%) and I_{NaCa} (S = -35%) moderately influence this electrophysiological property. Simulated values are smaller than experimentally reported [10].

Rate adaptation

On the one hand, our results show that $slope_{max,S1S2}$ is highly determined by I_{K1} (S = 125%), although I_{NaK} (S =47%) may also influence it. In this case, all our simulation results, but for G_{K1} reductions greater than 15%, are comprised in the electrophysiological range of this biomarker [11].
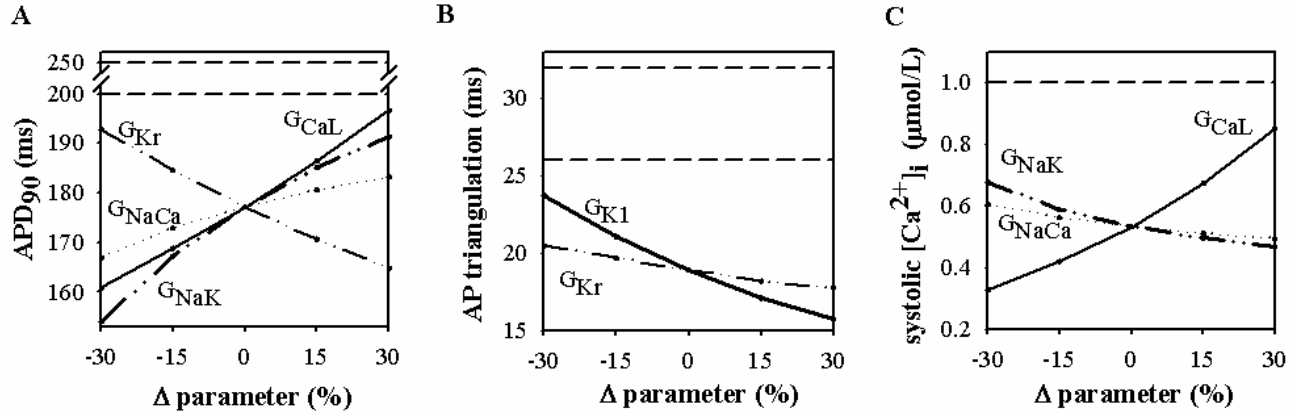
Figure 2. Percentual variations of steady state APD (A), AP triangulation (B) and systolic $[Ca^{2+}]_i$ (C) with changes in those relevant current conductances.
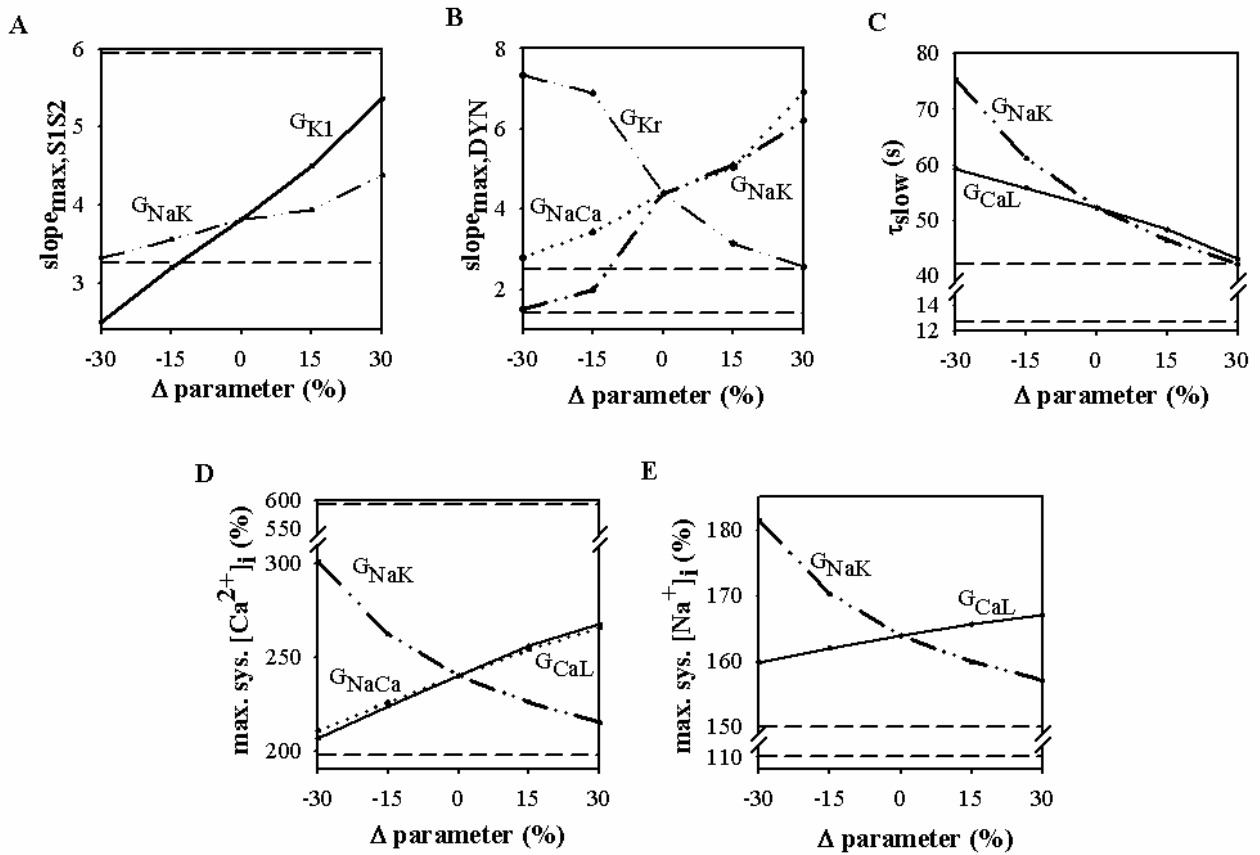

Figure 3. Percentual variations $slope_{max,S1S2}$ (A), $slope_{max,DYN}$ (B), τ_{slow} (C), maximum systolic $[Ca^{2+}]_i$ and maximum systolic $[Na^+]_i$ (D and E) respectively with changes in those relevant current conductances.

435

On the other hand, I_{Kr} (S = 182%), I_{NaK} (S = 179%) and I_{NaCa} (S = 157%) are key currents in slope$_{max,DYN}$ modulation. Results from our simulations are higher than experimentally reported [8]. However, it is difficult to quantitatively compare maximal restitution slopes computed in different investigations as they also depend on CI step and minium CI.

In addition, I_{NaK} (S = 106%) is essential in τ_{slow}, followed by I_{CaL} (S = -52%). Simulated τ_{slow}s are moderately longer than experimentally observed [12,13].

Finally, $[Ca^{2+}]_i$ and $[Na^+]_i$ rate dependence are markedly determined by I_{NaK} (S = 59% and 24%, respectively), although I_{CaL} (S = 42% and 7%, respectively) also plays a significant role. Indeed, these currents are directly involved in calcium and sodium regulation. As shown in Figure 3 panels D and E, control calcium rate dependence lies on the range of electrophysiological levels, although control sodium rate dependence is slightly higher [14,15].

4.   Discussion and conclusions

In this work, the Shannon et al. ventricular AP model [6] was used to investigate the ionic basis of the electrophysiological properties linked to arrhythmic risk in rabbit cardiomyocytes. Our simulations reveal that in rabbit, APD is moderately sensitive to changes in all repolarization current conductances, whereas AP triangulation is basically determined by I_{K1} and I_{Kr}. In addition, AP rate dependence is markedly dependent on I_{NaK}, I_{NaCa}, I_{Kr} and I_{CaL}. Furthermore, intracellular calcium and sodium concentrations are highly determined by I_{CaL}, I_{NaK} and I_{NaCa}. Most of these ionic mechanisms were qualitatively similar to human, although some differences were found.

Our results also show that standard APD restitution properties and calcium rate dependence are well reproduced by the model. Other properties, such as AP triangulation and steady state systolic $[Ca^{2+}]_i$ qualitatively resemble experimental observations, although quantitative differences with experimental recordings are observed.

Acknowledgements

References

[1] Lawrence CL, Pollard CE, Hammond TG, Valentin JP. Nonclinical proarrhythmia models: predicting Torsades de Pointes. J Pharmacol Toxicol Methods 2005; 52(1):46-59.

[2] Yap YG, Camm AJ. Drug induced QT prolongation and torsades de pointes. Heart 2003; 89(11):1363-1372.

[3] Bers DM, Despa S. Cardiac myocytes Ca2+ and Na+ regulation in normal and failing hearts. J Pharmacol Sci 2006; 100(5):315-322.

[4] Nolasco JB, Dahlen RW. A graphic method for the study of alternation in cardiac action potentials. J Appl Physiol 1968; 25(2):191-196.

[5] Pueyo E, Smetana P, Caminal P, de Luna AB, Malik M, Laguna P. Characterization of QT interval adaptation to RR interval changes and its use as a risk-stratifier of arrhythmic mortality in amiodarone-treated survivors of acute myocardial infarction. IEEE Trans Biomed Eng 2004; 51(9):1511-1520.

[6] Shannon TR, Wang F, Puglisi J, Weber C, Bers DM. A mathematical treatment of integrated Ca dynamics within the ventricular myocyte. Biophys J 2004; 87(5):3351-3371.

[7] Romero L, Pueyo E, Fink M, Rodriguez B. Impact of ionic current variability on human ventricular cellular electrophysiology. Am J Physiol Heart Circ Physiol 2009.

[8] Mahajan A, Sato D, Shiferaw Y, Baher A, Xie LH, Peralta R et al. Modifying L-type calcium current kinetics: consequences for cardiac excitation and arrhythmia dynamics. Biophys J 2008; 94(2):411-423.

[9] Guerard NC, Traebert M, Suter W, Dumotier BM. Selective block of IKs plays a significant role in MAP triangulation induced by IKr block in isolated rabbit heart. J Pharmacol Toxicol Methods 2008; 58(1):32-40.

[10] Chudin E, Goldhaber J, Garfinkel A, Weiss J, Kogan B. Intracellular Ca(2+) dynamics and the stability of ventricular tachycardia. Biophys J 1999; 77(6):2930-2941.

[11] Goldhaber JI, Xie LH, Duong T, Motter C, Khuu K, Weiss JN. Action potential duration restitution and alternans in rabbit ventricular myocytes: the key role of intracellular calcium cycling. Circ Res 2005; 96(4):459-466.

[12] Bell J, Rouze N, Krassowska W, Idriss S. The Electrocardiogram Restitution Portrait Quantifying Dynamical Electrical Instability in Young Myocardium. Comput Cardiol 2007; 34:789-792.

[13] Pitruzzello AM, Krassowska W, Idriss SF. Spatial heterogeneity of the restitution portrait in rabbit epicardium. Am J Physiol Heart Circ Physiol 2007; 292(3):H1568-H1578.

[14] Maier LS, Bers DM, Pieske B. Differences in Ca(2+)-handling and sarcoplasmic reticulum Ca(2+)-content in isolated rat and rabbit myocardium. J Mol Cell Cardiol 2000; 32(12):2249-2258.

[15] Despa S, Islam MA, Weber CR, Pogwizd SM, Bers DM. Intracellular Na(+) concentration is elevated in heart failure but Na/K pump function is unchanged. Circulation 2002; 105(21):2543-2548.

Address for correspondence

Lucía Romero Pérez
Universidad Politécnica de Valencia
Camino de Vera s/n
46071 Valencia
Spain
E-mail: lurope@doctor.upv.es